Journal of Materials Chemistry B

ROYAL SOCIETY OF CHEMISTRY

PAPER

View Article Online
View Journal | View Issue

Cite this: J. Mater. Chem. B, 2022, 10, 2853

Bio-mineralization of virus-like particles by metal–organic framework nanoparticles enhances the thermostability and immune responses of the vaccines†

Zhidong Teng,*[a] Fengping Hou,*[ac] Manyuan Bai,[a] Jiajun Li,[a] Jun Wang,[a] Jinen Wu,[a] Jiaxi Ru,[a] Mei Ren,[a] Shiqi Sun‡[a] and Huichen Guo‡[abd]

Received 10th December 2021,
Accepted 9th March 2022

DOI: 10.1039/d1tb02719k

rsc.li/materials-b

Virus-like particle (VLPs) vaccines have been extensively studied due to their good immunogenicity and safety; however, they highly rely on cold-chain storage and transportation. Nanotechnology of bio-mineralization as a useful strategy has been employed to improve the thermal stability and immunogenicity of VLPs. A zeolitic imidazole framework (ZIF-8), a core–shell structured nanocomposite, was applied to encapsulate foot-and-mouth disease virus (FMDV) VLPs. It was found that the ZIF-8 shell enhanced the heat resistance of VLPs and promoted their ability to be taken up by cells and escape from lysosomes. The VLPs-ZIF-8 easily activated antigen-presenting cells (APCs), triggered higher secretion levels of cytokines, and elicited stronger immune responses than VLPs alone even after being treated at 37 °C for 7 days. This platform has good potential in the development of VLP-based vaccine products without transportation.

Introduction

Foot-and-mouth disease (FMD) is a severe, highly contagious disease that infects cloven-hoofed animals. Its outbreak will cause enormous economic loss. At present, vaccines are still the most effective means to control and prevent the disease in many countries. Virus-like particles (VLPs) are composed of major structural proteins of virions without a viral genome. Thus, they are easily recognized and taken up by antigen-presenting cells (APCs) to trigger immune responses, exhibiting excellent immunogenicity and reactogenicity. Nowadays, VLPs have attracted widespread attention in the development of vaccines owing to their superior immunogenicity, good safety, and capacity to distinguish infected animals from immunized animals to eradicate FMDV.[1–4] So far, more than 110 VLP-based vaccines have been reported. VLP-based vaccines like hepatitis B virus (HBV) and human papillomavirus (HPV) have been approved and utilized to prevent related diseases.[4–6] Similar to native viruses, VLPs are required to be preserved at low temperatures to maintain their integrity and immune effectiveness. Therefore, almost all commercially available vaccines, including VLP-based ones, required constant refrigeration from production to delivery to guarantee the vaccine efficacy, which accounts for nearly eighty percent of the total cost of vaccines.[7,8] To this end, much effort has been devoted to enhancing the thermostability of vaccines to prolong the storage periods and reduce the dependence on cold-chain.

Biomimetic mineralization has been developed as an effective strategy for improving the thermal stability of vaccines. For instance, calcium mineralization has been used to protect VLPs.[9] With the advantages of facile synthesis, chemical robustness, thermostability, and biocompatibility, the use of metal–organic frameworks (MOFs) is promising as an alternative mineralization approach for the stabilization and delivery of proteins.[10–12] Specifically, Zn-based MOFs with methylimidazole as linkers have been reported as nanocarriers.[8,13] MOFs have been used to encapsulate some model proteins, such as bovine serum albumin (BSA), ovalbumin (OVA), and tobacco mosaic virus (TMV).[14–17] However, using MOFs as a mineralization strategy to improve the thermostability and immunogenicity is rarely reported in the development of VLPs-based vaccines.

Herein, we designed a zeolitic imidazole framework-8 (ZIF-8)-based biomimetic system that provided a framework

[a] State Key Laboratory of Veterinary Etiological Biology, National Foot-and-Mouth Disease Reference Laboratory, Lanzhou Veterinary Research Institute, Chinese Academy of Agricultural Sciences, Xujiaping 1, Lanzhou 730046, Gansu, P. R. China. E-mail: sunshiqi@caas.cn, guohuichen@caas.cn; Tel: 86-0931-8312213
[b] School of Animal Science, Yangtze University, Jingmi Street, Jingzhou District, Jingzhou 434025, P. R. China
[c] Molecular and Cellular Epigenetics (GIGA) and Molecular Biology (Gembloux Agro-Bio Tech), University of Liège (ULg), Avenue de l'Hôpital, 11, 4000 Liège, Belgium
[d] Yunnan Tropical and Subtropical Animal Virus Diseases Laboratory, Yunnan Animal Science and Veterinary Institute, Kunming, Yunnan, China

† Electronic supplementary information (ESI) available. See DOI: 10.1039/d1tb02719k

‡ These authors contributed equally to this work.

for protecting FMDV VLPs from environmental interference. VLPs-ZIF-8 composites were prepared *via* a facile one-pot biomimetic method and they showed outstanding biosafety and excellent stability at higher temperatures. The shell of VLPs-ZIF-8 also enabled VLPs to escape from lysosomes and release into the cytoplasm to trigger a good cellular immune response. The experiments *in vitro* and *in vivo* revealed that the biomimetic VLPs-ZIF-8 had excellent thermostability and induced strong humoral and cellular immune responses. We expect that the VLPs-ZIF-8 composite could shed light on the application of VLPs and ZIF-8 in the field of vaccines.

Experimental

Synthesis of ZIF-8 and VLPs-ZIF-8 composites

ZIF-8 and VLP-ZIF-8 composites were prepared in a pure aqueous system according to a modified procedure.[18] In brief, for the preparation of VLPs-ZIF-8, 2-methylimidazole aqueous solution (0.45 mL, 80 mM) and VLPs (100 μL, 1000 μg mL^{-1}) were quickly mixed, and then added to zinc nitrate solution (50 μL, 20 mM) and agitated together. After 10 min, a solution of 2-methylimidazole (0.45 mL, 80 mM) and zinc nitrate (50 μL, 20 mM) was quickly added and mixed,and further mineralization for 20 min. After ultrasonic dispersion, 2-methylimidazole (20 μL, 2 M) and zinc nitrate (5.5 μL, 200 mM) were added. After incubated for another 1 h, the composite was collected by centrifugation (8000 rpm, 10 min).

Dot blotting confirms VLP encapsulation

A nitrocellulose (NC) membrane was divided into 12 squares (1 × 1 cm), and the samples (ZIF-8, VLPs-ZIF-8, VLPs-ZIF-8 lysate and added VLPs) were added to each square with 7 μL per square. After natural drying, the NC membrane was blocked with 5% skimmed milk at room temperature (RT) for 1 h and then incubated with the primary antibody diluted with 1% skimmed milk (1 : 1000) at RT for 1 h. After being washed 5 times (10 min each time) with PBST solution, the NC membrane was incubated with an HRP-labeled anti-pig antibody diluted with 1% skimmed milk (1 : 2000) at RT for 1 h. Then the membrane was washed 5 times with PBST solution, and the VLPs were visualized through a luminous fluid.

Thermostability determination

1 mL of the sample (100 μg mL^{-1}) was treated at 45 °C (1, 3 and 6 h) and 60 °C (0.5, 1 and 3 h), respectively, to investigate the thermostability of VLPs and VLPs-ZIF-8 composites. VLPs and VLPs-ZIF-8 composites placed on ice were considered as controls. The samples were collected at a scheduled time and washed with purified water. After the samples were de-encapsulated, the protein released into the supernatant was collected by centrifugation (8000 rpm, 10 min). The protein content in the supernatant was measured using a Micro BCA assay. An ELISA was used to determine the protein activity of VLPs.

In vitro release of VLPs

The VLPs-ZIF-8 composite was dispersed in pH-modified solutions (pH7.4, 6.0, and 5.0) at 37 °C. The supernatant of the VLPs-ZIF-8 dispersion was collected by centrifugation (8000 rpm, 10 min) at different time intervals (0.5, 1, 2, 4, 6, and 8 h), and the released VLPs in the supernatant were detected using a BCA assay.

$$\text{Protein release ratio (\%)} = \frac{\text{Amount of VLPs in the supernatant}}{\text{The total amount of protein in VLPsZIF8}} \times 100\%$$

In vitro cytotoxicity

According to the manufacturer's protocol, an MTS assay was used to detect the cytotoxicity of ZIF-8, VLPs-ZIF-8, $Zn(NO_3)_2 \cdot 6H_2O$, or 2-methylimidazole. In brief, BHK-21 cells (1×10^4 cells $well^{-1}$) and PK-15 cells (1×10^4 cells $well^{-1}$) in 100 μL medium were seeded into 96-well plates, respectively. After 24 h, the cells were incubated with nanoparticles ZIF-8 and VLPs-ZIF-8 (from 0 μg mL^{-1} to 100 μg mL^{-1}, respectively), $Zn(NO_3)_2 \cdot 6H_2O$ or 2-methylimidazole (from 0 μg mL^{-1} to 600 μg mL^{-1}, respectively) for 24 h. Then the MTS reagent (Promega) was directly added to the cells and incubated for another 4 h. The absorbance at 490 nm was recorded using a microplate reader (Bio-Rad). The cell viability was calculated as follows:

$$\text{The cell viability (\%)} = \frac{\text{The average absorbance value of the experimental group}}{\text{The average absorbance value of the control group}} 100\%$$

Hemolysis assay

The blood of the mice was collected, and the red blood cells (RBCs) were collected by centrifugation (2000 rpm, 10 min). After being washed 5 times with PBS, the RBCs were diluted 10 fold with PBS. Simultaneously, VLPs-ZIF-8 was diluted with PBS to different concentrations, respectively. 0.3 mL of RBC solution were added to 1.2 mL of serially diluted VLPs-ZIF-8 to make the concentrations of VLPs-ZIF-8 25, 50, 100, 200, 400, 600, 800, and 1000 μg mL^{-1}, respectively. The diluted RBC solution was added to PBS or deionized water as a negative or positive control. The various mixed solutions were incubated at 25 ± 2 °C for 2 h. After centrifugation, the results were recorded by taking pictures, and the supernatant was collected. A UV-vis absorption spectrophotometer was used to record the absorbance of the supernatant to detect the hemolysis of RBCs in different concentrations of VLP-ZIF-8.

Results and discussion

Successful encapsulation of VLPs into the VLPs-ZIF-8 composite

FMDV VLPs were prepared by a self-assembly method established in our lab.[19] The purified proteins and digested proteins were detected by western blot. The results showed that the structural protein of FMDV (VP0, VP1, and VP3) was successfully

obtained (Fig. S1A, ESI†). The hydrated diameter of VLPs was mainly concentrated in the range of 30–40 nm (Fig. S1B, ESI†). The result indicated that the structural proteins were successfully assembled into VLPs.

VLPs-ZIF-8 composites were prepared through a facile one-pot biomimetic method in an aqueous solution. In the early synthesis process, it was found that the mineralization rate of FMDV VLPs was lower when 2-methylimidazole and Zn $(NO_3)_2 \cdot 6H_2O$ were added only once. According to the characteristics of the positive charge of VLPs-ZIF-8 and the negative charge of VLPs, the mineralization efficiency was improved by adding 2-methylimidazole and Zn $(NO_3)_2 \cdot 6H_2O$ repeatedly. The synthesized VLPs-ZIF-8 and pure ZIF-8 were characterized by transmission electron microscopy (TEM) and DLS. The TEM images of pure ZIF-8 (Fig. 1A) showed a uniform morphology with an average size of about 75 nm. It is noted that the VLPs-ZIF-8 composite exhibited a similar morphology, but the average size (~100 nm) was larger than that of ZIF-8 (Fig. 1B). Both particles showed good dispersibility and regular shape. DLS analysis showed that the ranges of hydrated particle sizes of ZIF-8 and VLPs-ZIF-8 were 75–100 and 95–120 nm, respectively (Fig. 1C). Because of the hydration, the size of the hydrated particles was larger than that of rigid particles.

Moreover, the zeta potentials of VLPs, ZIF-8, and VLPs-ZIF-8 were -8.83 ± 2.36 mV, 25.4 ± 2.8 mV, and 19.57 ± 2.3 mV, respectively, indicating that negatively charged VLPs were encapsulated by the positively charged ZIF-8. Further characterization was performed using Fourier transform infrared (FT-IR) spectroscopy and powder X-ray diffraction (PXRD). As shown in Fig. 1D, the FT-IR spectral data showed that the bands at 1648 cm^{-1} and 1536 cm^{-1} were observed in protein and the VLPs-ZIF-8 composite, which were ascribed to the amide I and II bands, respectively, indicating that VLPs were successfully encapsulated into VLPs-ZIF-8 composites. These characteristic bonds were not found in pure ZIF-8. In the PXRD patterns (Fig. 1E), the diffractions of the VLPs-ZIF-8 composite were almost identical to that of pure ZIF-8 in 2θ values except for a slight difference in intensity, suggesting that ZIF-8 coating VLPs did not affect its structure.[20] Successful encapsulation of VLPs in the VLPs-ZIF-8 composite was also evidenced by SDS-PAGE and western blot (Fig. S2, ESI†). Both SDS-PAGE and western blot results showed that the obvious protein bands (VP0, VP1, and VP3) in the VLPs-ZIF-8 composites were consistent with those in control VLPs. Furthermore, the mineralization efficiency of VLPs-ZIF-8 was about 63% (Fig. 1F), which was calculated by the protein amount according to the data of dot blot. The influence of different concentrations of 2-methylimidazole on the reactogenicity of VLPs was detected by an ELISA. The results showed that high concentrations of 2-methylimidazole reduced the reactogenicity of VLPs, but had little influence on VLP reactogenicity when the concentration of 2-methylimidazole was lower than 125 mM (Fig. S3, ESI†).

Encapsulation of VLPs with the ZIF-8 enhanced thermal stability of VLPs

Mineralization superiorly enhanced the thermal stability of proteins against denaturation. Therefore, time-dependent and temperature-dependent experiments were conducted to determine the thermal stability and reactogenicity of VLPs in the VLPs-ZIF-8 composite. The resultant VLPs-ZIF-8 composite and naked VLPs were treated with different temperatures (45 °C and 60 °C) and time periods (from 30 min to 6 h). Then the reactogenicity of the VLPs was measured by an ELISA. As shown in Fig. 2A, the activity of naked VLPs decreased sharply with an increase in temperature and

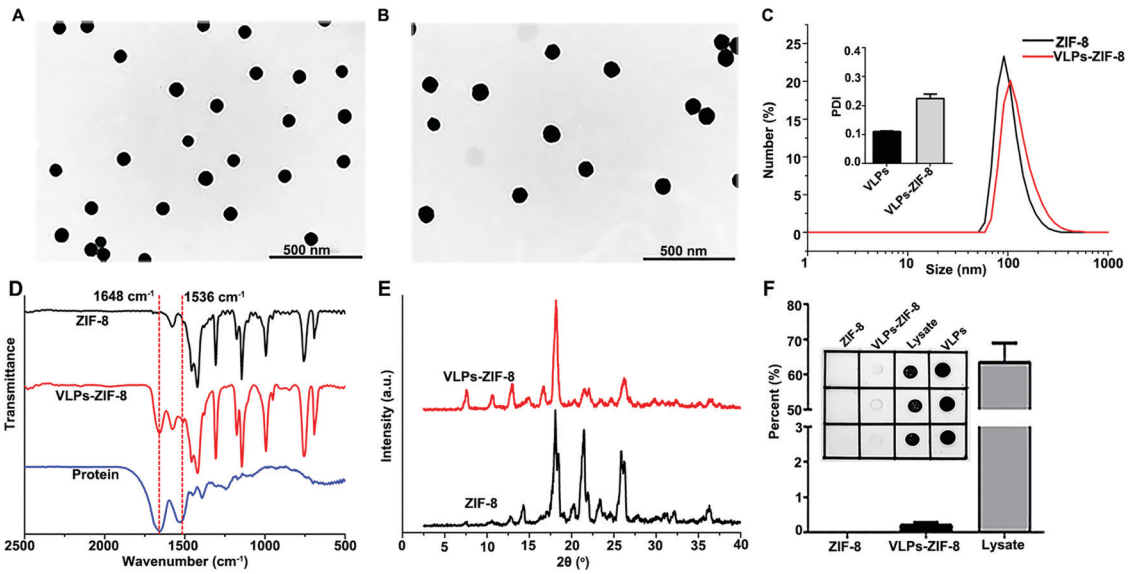

Fig. 1 Characterization of ZIF-8 and VLPs-ZIF-8. The TEM images of (A) ZIF-8 and (B) VLPs-ZIF-8. (C) The hydrated particle sizes and PDIs of samples (VLPs-ZIF-8 and ZIF-8) were measured by DLS. (D) FT-IR spectra of VLPs, ZIF-8 and VLPs-ZIF-8. (E) PXRD patterns of simulated ZIF-8 and VLPs-ZIF-8. (F) Dot blotting was used to detect the amount of VLPs bound to the surface of VLPs-ZIF-8 by electrostatic adsorption and the amount of encapsulated VLPs inside. The ratio of bound VLPs or encapsulated VLPs in VLPs-ZIF-8 was measured by gray scale analysis.

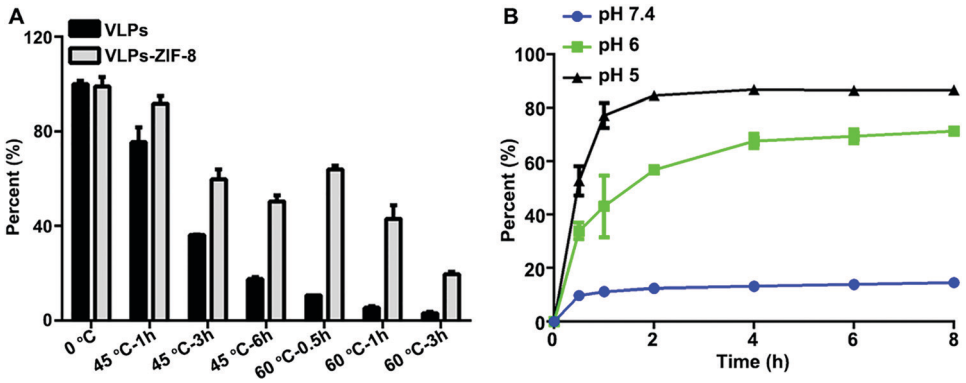

Fig. 2 Thermal stability and release at different pH values of VLPs. (A) The thermostability of VLPs-ZIF-8 was evaluated by detecting the reactogenicity at different temperatures (45 °C and 60 °C) for a designated time. (B) VLPs released from VLPs-ZIF-8 at different pH values.

time during the treatment. In contrast, the percentage of activity retention in the VLPs-ZIF-8 composite was significantly higher than that of bare VLPs at high temperatures. The results showed that the activity of VLPs remained 50% after VLPs-ZIF-8 were treated at 45 °C for 6 h, while the activity of VLPs in the VLPs-ZIF-8 composite remained 60% after being treated at 60 °C for 0.5 h. However, the activity was about 10% after naked VLPs were treated at 60 °C for 0.5 h. Therefore, under the protection of ZIF-8 biomineralization, the thermal stability and activity of VLPs were improved, providing a useful strategy to solve the issues associated with cold-chain transportation.

Release of VLPs in VLPs-ZIF-8 composites at different pH

When vaccines trigger immune responses, they will experience different physiological environments, including the neutral environment of body fluids and the acidic environment of cell lysosomes. Therefore, the different pH values were set to imitate physiological environments *in vitro* to verify whether VLPs in VLPs-ZIF-8 composites could be released. As shown in Fig. 2B, VLPs-ZIF-8 composites showed a slow release at pH 7.4, and less than 20% of VLPs were released after being treated at 37 °C for 8 h. In contrast, the release rate of VLPs was significantly increased with decreased pH values. About 55% of VLPs were released from the VLPs-ZIF-8 composite at pH 6.0 after being treated for 2 h, while it only took 0.5 h at pH 5.0 to reach the same amount. The result of pH-sensitive antigen release was consistent with those in the literature results.[21] ZIF-8 is stable under neutral conditions but decomposes faster under acidic conditions due to imidazole protonation.[17,22] The result indicated that the composites were relatively stable in a neutral environment, but the encapsulated proteins were quickly released in an acidic environment, which resulted in the increase of antigen capture and presentation by APCs, triggering strong immune responses.

Stability of VLPs-ZIF-8 in different solutions

The stability results of VLPs-ZIF-8 in different solutions showed that the antigen release of VLPs-ZIF-8 in deionized water solution was lower, and the release gradually increased with time in normal saline, DMEM, or simulated body fluid (SBF) solution (Fig. S4, ESI†).

Good biocompatibility of ZIF-8 and VLPs-ZIF-8

The biocompatibility of nanomaterials is one of the main problems to be considered as vaccine adjuvants. An MTS assay was employed for BHK-21 cells (Fig. 3A) and PK-15 cells (Fig. 3B) to evaluate the cytotoxicity of ZIF-8 and VLPs-ZIF-8. Though obvious cytotoxicity was observed when the concentration of ZIF-8 nanoparticles reached 100 μg mL^{-1}, the viability of the cells treated with VLPs-ZIF-8 nanocomposites was more than 75% at the same concentration, displaying low cytotoxicity compared to ZIF-8. Meanwhile, BHK-21 cells and PK-15 cells were incubated with different concentrations of $Zn(NO_3)_2{\cdot}6H_2O$ or 2-methylimidazole to elucidate this phenomenon. The results showed that cytotoxicity was mainly triggered by $Zn(NO_3)_2{\cdot}6H_2O$ (Fig. S5, ESI†), which could induce necrocytosis at a high concentration.[23] It was known that the hemolysis behaviour of nanoparticles was a significant indicator to evaluate their biocompatibility. Therefore, mice red blood cells (RBCs) were added to the VLPs-ZIF-8 suspension with different concentrations (ranging from 25 to 1000 μg mL^{-1}). The results of the hemolysis assay (Fig. 3C) showed that even 400 μg mL^{-1} VLPs-ZIF-8 did not cause significant hemolysis, which revealed that the injection of VLPs-ZIF-8 into the animal body would not cause hemolysis. The hemoglobin release from RBCs was also detected by UV-Vis spectroscopy (Fig. 3D), and the results were consistent with the hemolysis assay. The result of hemolysis also suggested that the nanocomposite has good biocompatibility. Owing to the excellent biocompatibility *in vivo* and *in vitro*, VLPs-ZIF-8 has great potential as a novel vaccine.

Encapsulation of VLPs with ZIF-8 enhanced the cellular uptake of antigens

The easier the APCs take up the antigens, the more likely they elicit strong immune responses. Most of the antigens combined with the nanoparticles as a delivery system can significantly enhance the efficiency of antigen uptake.[24,25] We have demonstrated that the zeta potentials of VLPs changed from negative to positive after being wrapped by ZIF-8.

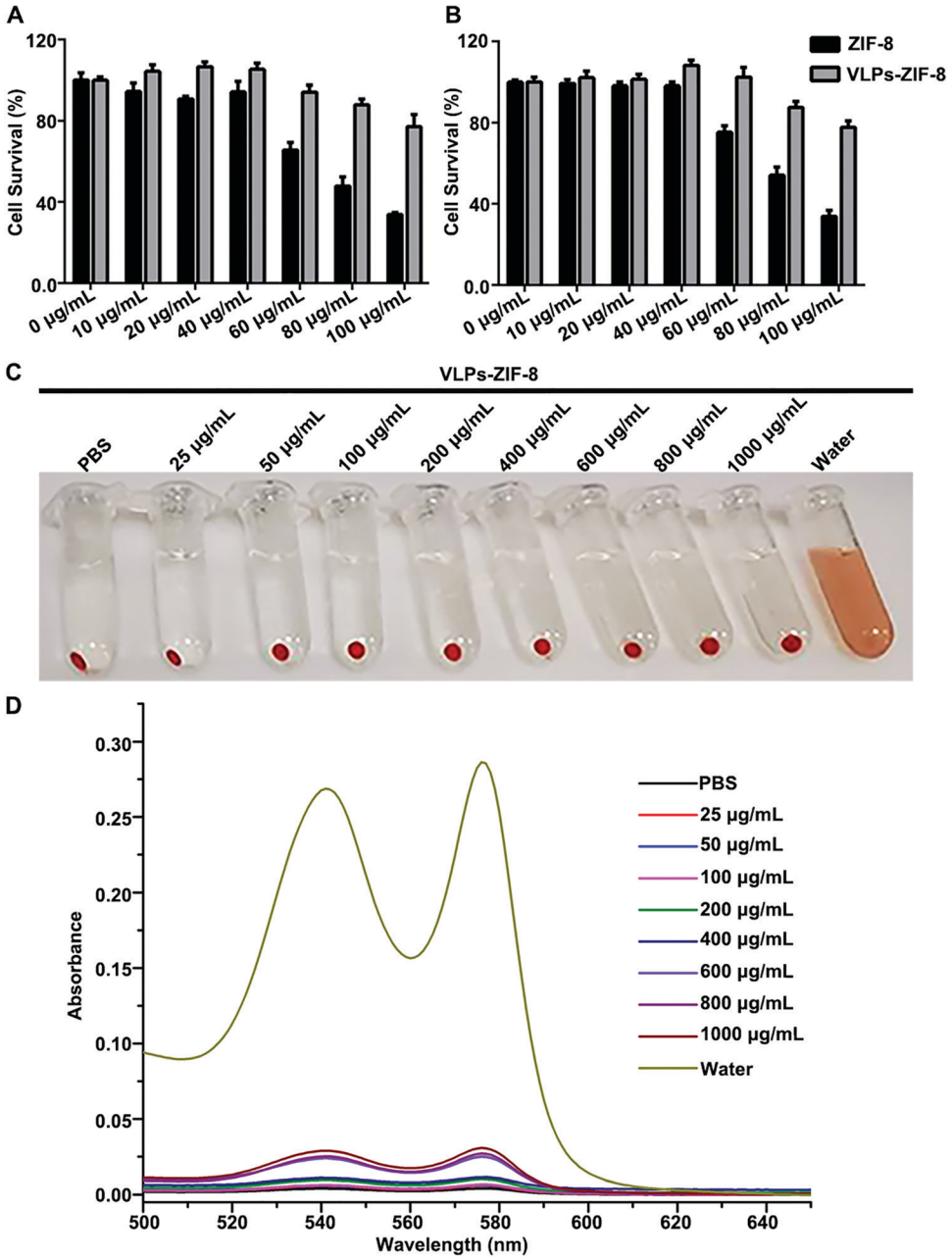

Fig. 3 Biocompatibility of ZIF-8 and VLPs-ZIF-8. Cell viability based on the MTS assay of (A) BHK-21 cells and (B) PK-15 cells treated with various concentrations of ZIF-8 or VLPs-ZIF-8. (C) Photos of the hemolysis assay. (D) The absorption peak of hemoglobin in the supernatant of RBCs treated with different concentrations of VLPs-ZIF-8 was measured by UV-Vis.

The positive charge of VLPs-ZIF-8 is advantageous for binding to the negatively charged cell membrane and subsequent cellular uptake.[28] The cellular uptake efficiency of antigens was further investigated by comparing the bare VLPs with the VLPs-ZIF-8 composites. The indirect immunofluorescence assay demonstrated that the uptake of VLPs by BHK-21 cells was time-dependent, and the uptake of VLPs-ZIF-8 was significantly higher than that of the naked VLPs (Fig. 4A). Furthermore, the uptake level of VLPs-ZIF-8 by BHK-21 and RAW264.7 cells was also measured by western blot. As shown in Fig. 4B and C, the amount of VLPs taken up by the cells incubated with VLPs-ZIF-8 was higher than that taken up by the cells incubated with bare VLPs. The cell uptake experiment results proved that the positively charged VLPs-ZIF-8 was more easily taken up by the cells, which might be favourable for triggering good immune responses.

Encapsulation with ZIF-8 assisted VLP escape from lysosomes

More interestingly, it has been reported that the ligand of 2-methylimidazole can be easily protonated in an acidic lysosome microenvironment, leading to the so-called proton sponge effect that induces extensive inflow of ions/water and eventually lysosomal membrane rupture.[22,26] This may also cause the dissociation

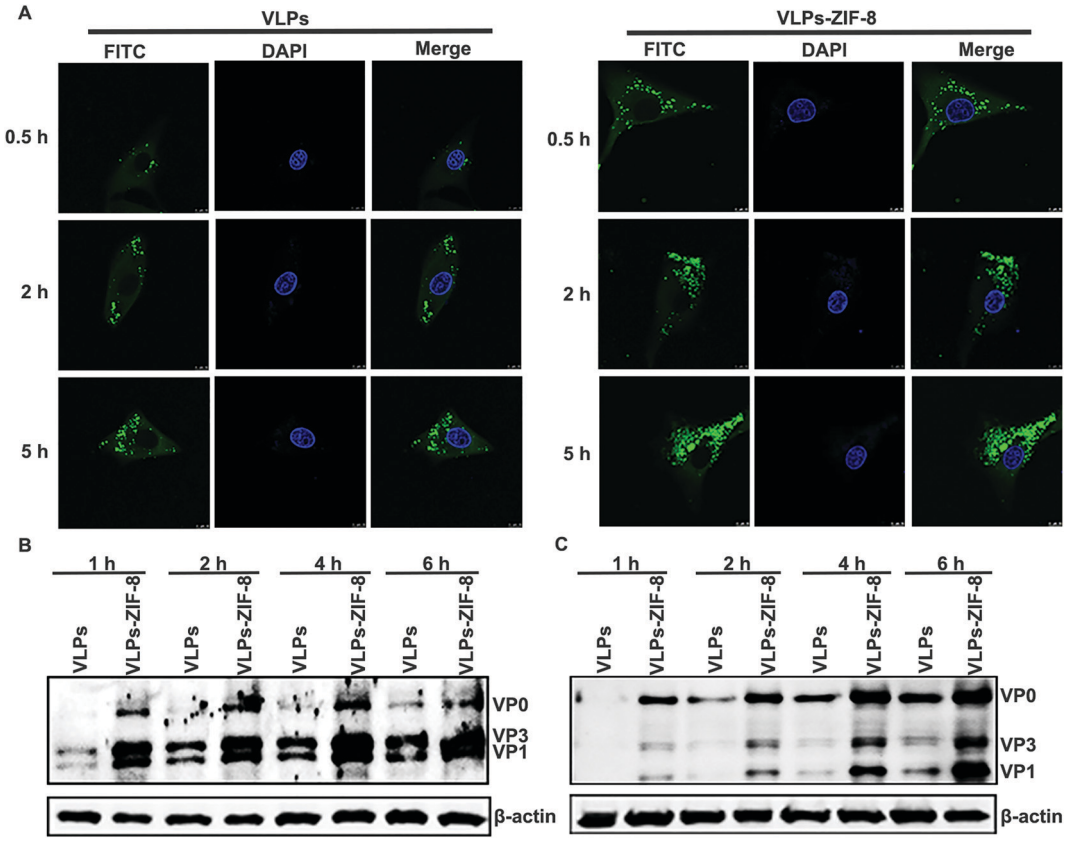

Fig. 4 The cellular uptake of VLPs-ZIF-8. (A) The amount of VLPs taken up by BHK-21 cells was visualized by laser confocal microscopy. BHK-21 cells were incubated with VLPs-ZIF-8 or VLPs for different times (0.5 h, 2 h and 5 h). Then they were stained with polyclonal pig anti-FMDV antibody and FITC-conjugated goat anti-pig igg (green). Nuclei were stained with DAPI (blue). The amount of VLPs ingested by (B) BHK-21 cells and (C) RAW264.7 cells were measured using western blotting.

of ZIF-8 and fast antigen release, facilitating antigen escape from lysosomes and antigen presentation by a major histocompatibility complex (MHC) class I molecule to prime the $CD8^+$ T response.[27–29] Therefore, BHK-21 cells were incubated with VLPs-ZIF-8 composites at different periods (0.5, 2, and 5 h), and then examined by confocal laser scanning microscopy (CLSM) to determine whether the antigen escaped from endolysosomes. The overlapping (yellow) of red fluorescence from the lysosome and green fluorescence from VLPs indicated the entrapment of VLPs-ZIF-8 in the lysosome. The CLSM images showed that an increasing amount of VLPs-ZIF-8 composites were absorbed by the cells and entered into lysosomes from 0.5 h to 2 h (Fig. 5), indicating efficient internalization of the nanocomposites with time. When the incubation time extended to 5 h, less overlapped yellow fluorescence and more green fluorescence were observed compared to 2 h, suggesting that more VLPs escaped from lysosomes to the cytoplasm. The results of the lysosomal escape experiment confirmed that VLPs encapsulated with ZIF-8 could promote lysosomal antigen escape. Therefore, the ZIF-8 biomineralization strategy is expected to play an important role in the VLPs vaccine to induce a strong cellular immune response.

VLPs-ZIF-8 highly activated APCs

Macrophages and DCs are professional APCs that play significant roles in innate and adaptive immune responses. Macrophages can recognize and destroy foreign antigens that promote inflammatory responses. The immunostimulatory cytokines secreted by APCs such as macrophages and DCs are regarded as indicators of immune response activation.[30–32] Tumour necrosis factor-α (TNF-α) is an inflammatory cytokine produced by monocytes and macrophages, which fights against infection.[33] Meanwhile, interleukin-6 (IL-6) is also a key cytokine that regulates acute inflammatory responses and plays an important role in regulating T lymphocyte activation and differentiation.[34] RAW264.7 macrophages and DCs were treated with VLPs, ZIF-8, VLPs-ZIF-8, LPS and PBS to investigate whether cytokine secretion was promoted during cell maturation. As shown in Fig. 6A and B, both ZIF-8 and VLPs-ZIF-8 induced higher IL-6 and TNF-α than the PBS group, while their levels in the VLPs-ZIF-8 group were significantly higher than those in the VLP group. The elevated levels of TNF-α and IL-6 in Raw264.7 macrophages indicated that VLPs-ZIF-8 could induce an inflammatory response and improve immune stimulatory activity. DCs have long cytoplasmic protrusions, activating the initial T cells to proliferate and exerting immune effects. The differentiation of T cells is strongly related to the secretion of cytokines. It is reported that IL-12p70 is a key Th1-driving cytokine, which contributes to the activation of $CD8^+$ T cells, triggering the cellular immune response.[35,36] The cytokine secretion from DCs showed that the VLPs-ZIF-8 nanocomposite also elicited a higher level of IL-12p70 than the VLPs group, which

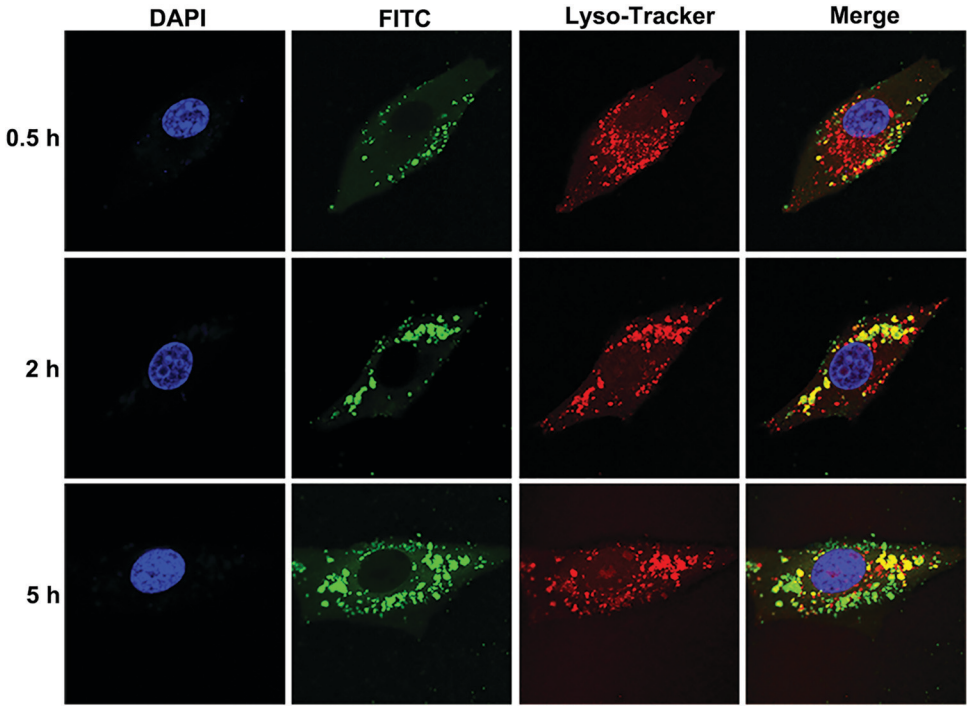

Fig. 5 Lysosomal escape of VLPs-ZIF-8. VLPs encapsulated by ZIF-8 escaped from lysosomes in BHK-21 cells.

was even higher than the positive control, lipopolysaccharide (LPS) group (Fig. 6C), suggesting that VLPs-ZIF-8 was easier to activate cellular immune responses.

Histopathological and biochemical index evaluation

Histopathological assessment was implemented to examine the possible damage to tissues and organs caused by vaccine formulations. Organs of the heart, liver, spleen, lungs, and kidneys were collected from mice inoculated with PBS, VLPs, VLPs-ZIF-8, and VLPs-ISA206, respectively. As shown in Fig. 7, there were no lesions in the tissues of mice immunized with VLPs-ZIF-8, compared to the control groups after the hematoxylin and eosin (H&E) stain, which implied that the immunized dose of VLPs-ZIF-8 could be utilized on the mice without causing body damage. The blood of mice in different immunization groups (VLPs group, VLPs-ZIF-8 group, VLPs-ISA206 group) was collected, the serum was separated, and the influence of different immunization agents on the mice was observed by measuring biochemical indicators. The results are shown in Table S1 (ESI†), the levels of aspartate aminotransferase, creatine kinase, creatinine, and total bilirubin in the VLPs, VLPs-ZIF-8 and VLPs-ISA206 groups were within the normal range, indicating that different immunization groups did not affect the biological indicators of mice, which further proved that each immunized substance had good biocompatibility.

Biodistribution of VLPs-ZIF-8

The zinc contents of the main organs (heart, liver, spleen, lungs, and kidneys) of mice injected with VLPs-ZIF-8 *via* the tail vein and of non-injected mice were detected by ICP-MS. As shown in Fig. S6 (ESI†), 48 hours after injection, the zinc content increased significantly in the heart, liver and kidneys, increased in the spleen, and almost no increase in the lungs, indicating that after VLPs-ZIF-8 entered the blood circulation, part of it entered the liver and kidneys for excretion, and part of it was retained in the spleen.

Encapsulation with ZIF-8 boosted immune responses induced by VLPs

The adjuvant effect of ZIF-8 and the thermal protection effect on VLPs were further verified by immunizing mice. The immune response of VLPs, VLPs-ZIF-8, and VLPs-ISA206 with or without heat treatment (37 °C for 7 days) was investigated. Female BALB/c mice were immunized with VLPs, VLPs-ZIF-8, VLPs-ISA206, VLPs-heat, VLPs-ZIF-8-heat, VLPs-ISA206-heat, and PBS by intramuscular injection, respectively. All the mice remained healthy, and their weights were within the normal range throughout the experiment (Fig. 8A). Sera were collected at 28 days post-immunization to detect the specific antibody level. The specific antibody level produced by mice immunized with VLPs-ZIF-8 was not significantly different from the VLPs group (Fig. 8B). It is worth noting that the specific antibody titers showed no significant difference between the heat-treated and untreated mice in the VLPs-ZIF-8 group. However, significant differences were observed in both the VLPs and VLPs-ISA206 groups with or without heat treatment (Fig. 8B). The data *in vivo* were consistent with the thermal stability tests *in vitro*, which verified that the biomimetic mineralization of VLPs with good thermostability facilitated strong immune responses. To further verify the immunostimulatory activity, total IgG1 and IgG2a were

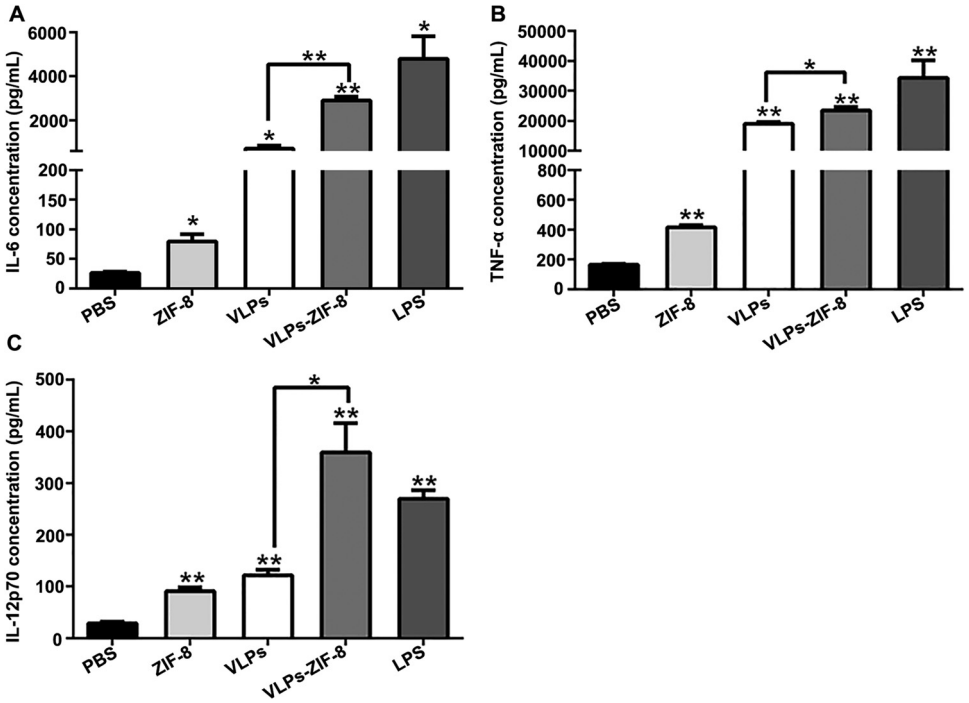

Fig. 6 VLPs-ZIF-8 promotes the activation of antigen presenting cells. Cytokine secretion of IL-6 (A), TNF-α(B) after RAW264.7 cells were incubated with PBS, ZIF-8, VLPs, VLPs-ZIF-8 and LPS for 12 h, and IL-12p70 (C) after DCs were incubated with PBS, ZIF-8, VLPs, VLPs-ZIF-8 and LPS for 12 h. * $0.01 \leq p < 0.05$, ** $p < 0.01$, ns: no significant difference.

tested using an ELISA. The IgG1 and IgG2a produced by immunized sera can reflect the level of immune response and indicate the type of immune response triggered by the vaccine. The levels of IgG1 and IgG2a in the group immunized with VLPs-ZIF-8 were significantly higher than the VLPs group (Fig. S7A and B, ESI†). The difference between the VLPs-ZIF-8 group and the VLPs-ISA206 group was not significant. Interestingly, the ratio of IgG2a/IgG1 induced by VLPs-ZIF-8 was significantly higher than those of the VLPs and VLPs-ISA206 immunized groups, respectively. However, there was no statistical difference in the ratio of IgG2a/IgG1 between the VLPs-ISA206 immunized group and the VLPs immunized group (Fig. S7C, ESI†). The ratio

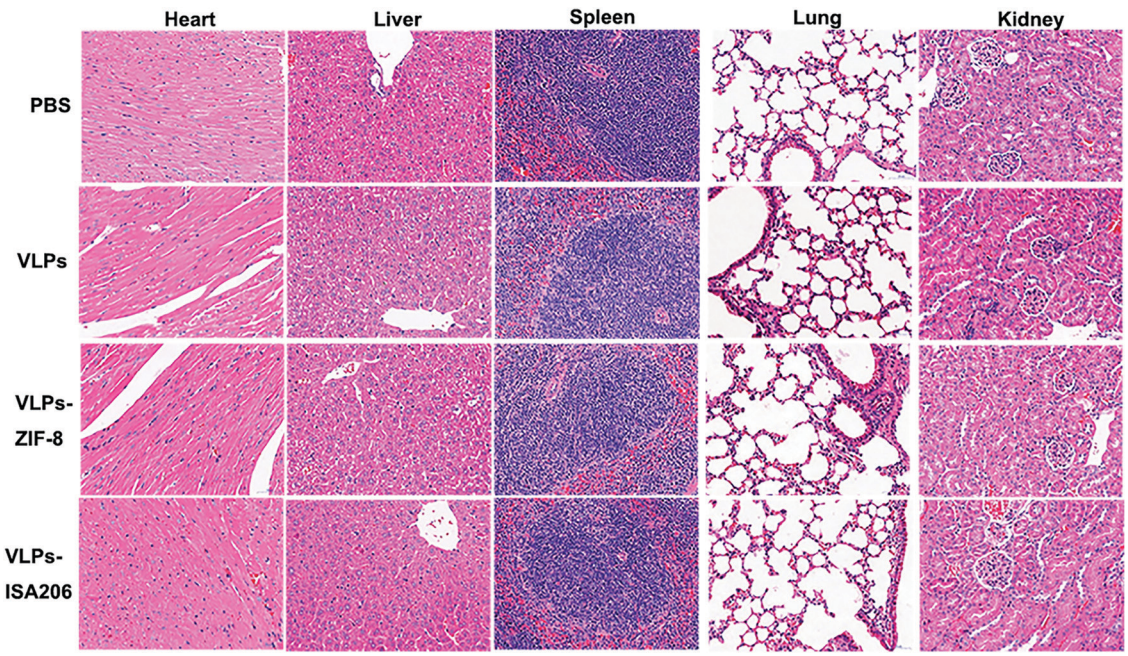

Fig. 7 Histopathological evaluation. Hematoxylin & Eosin (H&E) staining of vaccine injected mice tissue showed no obvious damage.

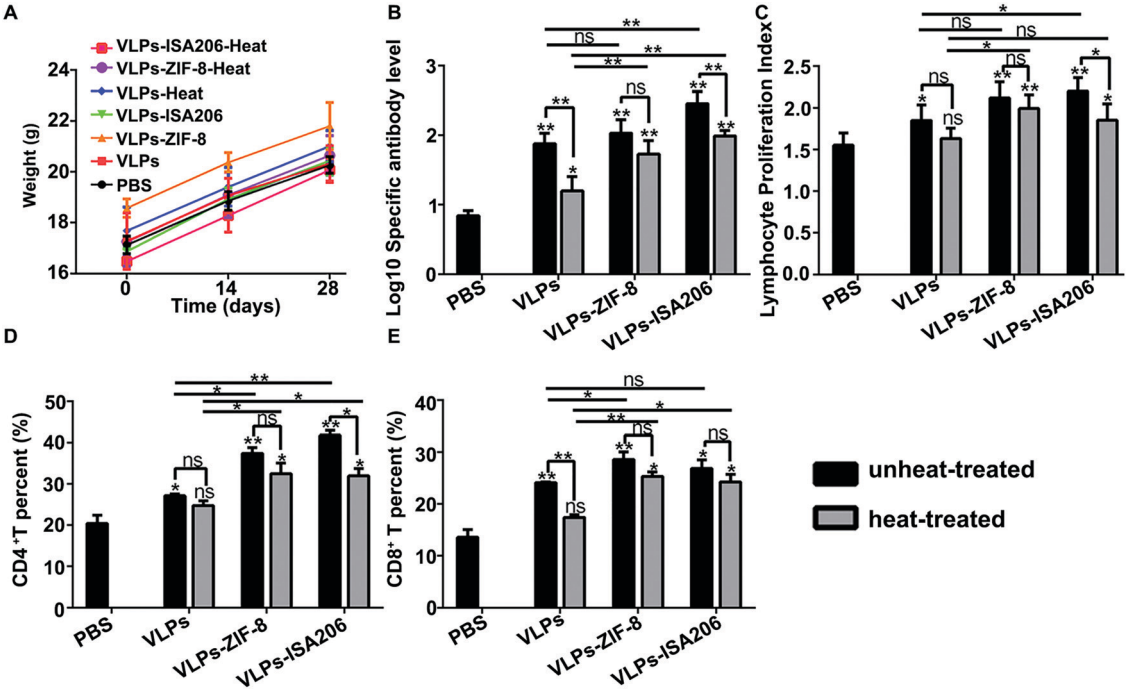

Fig. 8 Immune responses induced by VLPs-ZIF-8. (A) The weight changes of mice. The body weights of immunized mice was weighed at 0, 14, and 28 days after immunization. (B) Specific antibody levels in the mice immunized with various vaccine formulations. (C) Proliferative responses of splenocytes restimulated by antigen *in vitro*. Flow cytometry results of CD4+ T (D) and CD8+ T (E) cells in splenocytes harvested from mice immunized after 28 days. Each group contains two subgroups, untreated vaccine groups (black column) and heat-treated vaccine group (gray column), respectively, except for the PBS control group. Error bars indicate SD. * $0.01 \leq p < 0.05$ and ** $p < 0.01$; ns: no significant difference.

of IgG2a/IgG1 can better reflect the Th1-based immune response level.[37] The results of IgG2a/IgG1 indicated that ZIF-8 mineralization of VLPs could significantly enhance the Th1 immune response, which could be attributed to the high cellular uptake efficiency, sustained pH-responsive release, and lysosomal escape. The splenocyte proliferation assay was conducted to validate that the immune system can be stimulated and respond to a second exposure to the same antigen quickly and effectively. Splenocytes collected from mice immunized with VLPs-ZIF-8 proliferated more efficiently than the VLPs group (Fig. 8C). The heat-treated VLPs-ZIF-8 composite displayed a negligible difference from the non-heat-treated VLPs-ZIF-8 group. However, the splenocyte proliferation index of heat-treated VLPs and VLPs-ISA206 was significantly different from that of untreated ones (Fig. 8C). Therefore, the thermally stable VLPs-ZIF-8 nanocomposite could maintain a good specific memory response after heat treatment. $CD4^+$ T and $CD8^+$ T cells are two major lymphocyte subsets in adaptive immune responses. After being activated, naïve $CD4^+$T cells differentiate into different subsets called Th1, Th2, and Th17 cells, which activate B cells or CTLs to elicit an immune response. $CD8^+$ T cells are mainly involved in the cellular immune response.[38,39] The frequency of $CD4^+$ T cells and $CD8^+$ T cells was then measured by flow cytometry. Mice immunized with VLPs-ZIF-8 displayed higher percentages of $CD4^+$ T cells (Fig. 8D and Fig. S8, ESI†) and $CD8^+$ T cells (Fig. 8E and Fig. S9, ESI†) than the PBS group and the VLPs group. The group immunized with bare VLPs showed a lower T cell response, presumably due to the degradation and insufficient cellular uptake capacity.[40] Unlike VLPs-ZIF-8, either the VLPs group or the VLPs-ISA206 group showed relatively significant decreases after heat treatment. The results of lymphocyte typing showed that the $CD4^+$ T cells and $CD8^+$ T cells of the VLPs-ZIF-8 immunized group were significantly higher than the VLPs group before and after heat treatment, which showed that ZIF-8 as an adjuvant for the VLPs vaccine promotes not only cellular and humoral immune responses but also has a thermal-protection effect on antigens.

The cytokine levels of splenocytes in different immune groups

Since we observed that MOF-encapsulated vaccines induced a Th1-biased antibody response in mice compared to the antigen alone, we further investigated the cytokine levels secreted by splenic lymphocytes of immunized mice. Inflammatory cytokines such as TNF-α and IL-6 regulate the growth and differentiation of various cells and play important regulating roles in immunity.[33,34] IFN-γ, a Th1 cytokine, is essential to promote the cellular immune response, which is significant for responding to viral infections and eliciting the differentiation of CTLs from $CD8^+$ T cell precursors.[41,42] IL-4, a Th2 cytokine, is closely related to the humoral immune response.[43,44] The cytokine (IFN-γ, IL-4, TNF-α, and IL-6) levels in the supernatants of the splenocyte cultures were tested using ELISA kits according to the manufacturer's instructions. The results showed that the secretion of cellular immune-related cytokines, such as IFN-γ, elicited by the VLPs-ZIF-8 nanocomposite was higher than that in other groups (Fig. 9A). Interestingly, the secretion levels of humoral immunity-related cytokine IL-4 (Fig. 9B) and inflammation-related cytokines TNF-α

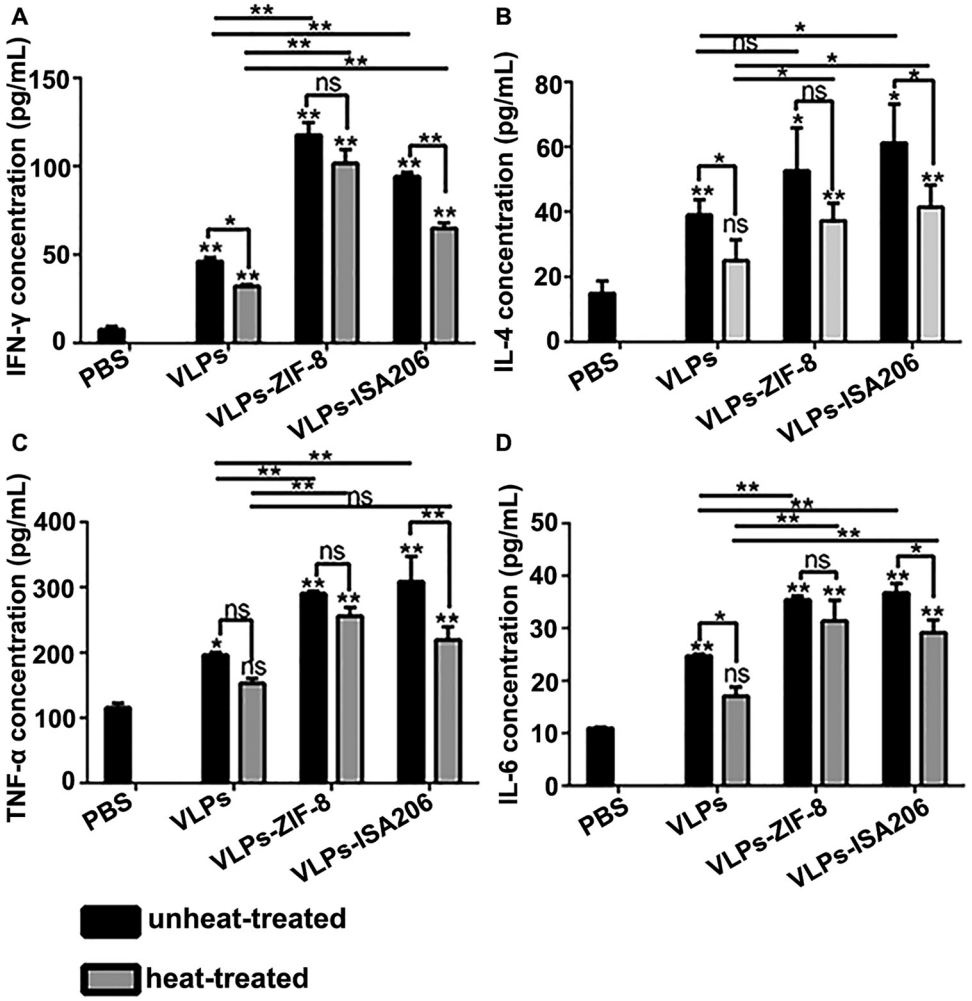

Fig. 9 Cytokine levels of splenocytes in different immune groups. The levels of IFN-γ (A), IL-4 (B), TNF-(C) and IL-6 (D) secreted by splenocytes after the mice were immunized for 28 days. Each group contains two subgroups, untreated vaccine groups (black column) and heat-treated vaccine group (gray column), respectively, except for the PBS control group. Error bars indicate SD. * 0.01 Ôëñ$p < 0.05$ and **$p < 0.01$; ns: no significant difference.

(Fig. 9C) and IL-6 (Fig. 9D) in the VLPs-ZIF-8 immunized group were relatively higher than those in the VLPs and PBS groups. The results showed that ZIF-8 mineralized VLPs had enhanced Th1 and Th2 type immune responses. It was also observed that the secretion of all cytokines stimulated by the heat-treated VLPs-ZIF-8 nanocomposite showed no significant difference compared to the untreated group, in contrast to the VLPs group, which showed lower secretion of cytokines after heat treatment, except for the secretion of TNF-α. Altogether, the bio-mineralized VLPs-ZIF-8 nanocomposite effectively enhanced the heat resistance of VLPs and protected them against degradation, and further elicited both humoral and cellular immunity, which is beneficial for the preparation of effective thermostable vaccines.

Conclusions

In summary, we have developed a novel platform in which antigen VLPs were encapsulated into ZIF-8 to prepare thermostable vaccines. This biomimetic mineralization strategy is a facile one-pot process with high encapsulation efficiency. The resultant VLP-ZIF-8 composite has excellent biocompatibility, without obvious damage to organs. Importantly, VLP-ZIF-8 showed improved thermostability and retained the immunogenicity after being treated at 37 °C for 7 days. Moreover, ZIF-8 encapsulation promoted cellular uptake and lysosomal escape. Thus both the humoral immunity and cellular immunity were enhanced. Therefore, the bio-mineralization strategy of VLPs is promising for producing thermostable vaccines with enhanced immune responses, paving the way for the development of next-generation vaccines with high performance and avoiding cold chain storage and transportation.

Author contributions

Conceptualisation: Huichen Guo, Shiqi Sun, and Zhidong Teng; writing-original draft: Zhidong Teng and Fengping Hou; writing-review and editing: Fengping Hou, Zhidong Teng,

Huichen Guo, Shiqi Sun, Mei Ren, and Jiaxi Ru; experiments: Zhidong Teng, Fengping Hou, Manyuan Bai, Jiajun Li, Jun Wang, Mei Ren, and Jinen Wu; formal analysis: Zhidong Teng and Jiajun Li; and supervision: Shiqi Sun, Jinen Wu, and Jiaxi Ru; all authors discussed the results and commented on the manuscript. All authors have read and agreed to the published version of the manuscript.

Conflicts of interest

The authors of this paper declared no financial conflict of interest.

Acknowledgements

This work was supported by grants from the National Key Research and Development Program (2021YFD1800300) and the National Natural Science Foundation of China (32002272, 31873023, 32072847, and 32072859).

References

1 R. Noad and P. Roy, *Trends Microbiol.*, 2003, **11**, 438–444.
2 L. M. M. Neto, A. Kipnis and A. P. Junqueira-Kipnis, *Front. Immunol.*, 2017, **8**, 239, DOI: 10.3389/fimmu.2017.00239.
3 B. Chackerian, *Expert Rev. Vaccines*, 2007, **6**, 381–390.
4 F. Liu, S. Ge, L. Li, X. Wu, Z. Liu and Z. Wang, *Res. Vet. Sci.*, 2012, **93**, 553–559.
5 E. V. L. Grgacic and D. A. Anderson, *Methods*, 2006, **40**, 60–65.
6 C. Ludwig and R. Wagner, *Curr. Opin. Biotechnol.*, 2007, **18**, 537–545.
7 K. Park, *J. Controlled Release*, 2011, **152**, 329.
8 R. Ricco, W. B. Liang, S. B. Li, J. J. Gassensmith, F. Caruso, C. Doonan and P. Falcaro, *ACS Nano*, 2018, **12**, 13–23.
9 P. Du, R. H. Liu, S. Q. Sun, H. Dong, R. B. Zhao, R. K. Tang, J. W. Dai, H. Yin, J. X. Luo, Z. X. Liu and H. C. Guo, *Nanoscale*, 2019, **11**, 22748–22761.
10 D. L. Shen, A. Y. Pang, Y. F. Li, J. Dou and M. D. Wei, *Chem. Commun.*, 2018, **54**, 1253–1256.
11 M. X. Wu and Y. W. Yang, *Adv. Mater.*, 2017, **29**, 1606134.
12 H. Y. Zhang, J. Zhang, Q. Li, A. X. Song, H. L. Tian, J. Q. Wang, Z. H. Li and Y. X. Luan, *Biomaterials*, 2020, **245**, 119983.
13 S. Rojas, F. J. Carmona, C. R. Maldonado, P. Horcajada, T. Hidalgo, C. Serre, J. A. R. Navarro and E. Barea, *Inorg. Chem.*, 2016, **55**, 2650–2663.
14 T. T. Chen, J. T. Yi, Y. Y. Zhao and X. Chu, *J. Am. Chem. Soc.*, 2018, **140**, 9912–9920.
15 M. A. Luzuriaga, R. P. Welch, M. Dharmarwardana, C. E. Benjamin, S. B. Li, A. Shahrivarkevishahi, S. Popal, L. H. Tuong, C. T. Creswell and J. J. Gassensmith, *ACS Appl. Mater. Interfaces*, 2019, **11**, 9740–9746.
16 Y. Yang, Q. Q. Chen, J. P. Wu, T. B. Kirk, J. K. Xu, Z. H. Liu and W. Xue, *ACS Appl. Mater. Interfaces*, 2018, **10**, 12463–12473.
17 X. F. Zhong, Y. T. Zhang, L. Tan, T. Zheng, Y. Y. Hou, X. Y. Hong, G. S. Du, X. Y. Chen, Y. D. Zhang and X. Sun, *J. Controlled Release*, 2019, **300**, 81–92.
18 G. Cheng, W. Li, L. Ha, X. Han, S. Hao, Y. Wan, Z. Wang, F. Dong, X. Zou, Y. Mao and S. Y. Zheng, *J. Am. Chem. Soc.*, 2018, **140**, 7282–7291.
19 H. C. Guo, S. Q. Sun, Y. Jin, S. L. Yang, Y. Q. Wei, D. H. Sun, S. H. Yin, J. W. Ma, Z. X. Liu, J. H. Guo, J. X. Luo, H. Yin, X. T. Liu and D. X. Liu, *Vet. Res.*, 2013, **44**, DOI: 10.1186/1297-9716-44-48.
20 Y. Zhang, F. M. Wang, E. G. Ju, Z. Liu, Z. W. Chen, J. S. Ren and X. G. Qu, *Adv. Funct. Mater.*, 2016, **26**, 6454–6461.
21 T. T. Chen, J. T. Yi, Y. Y. Zhao and X. Chu, *J. Am. Chem. Soc.*, 2018, **140**, 9912–9920.
22 H. Q. Zheng, Y. N. Zhang, L. F. Liu, W. Wan, P. Guo, A. M. Nystrom and X. D. Zou, *J. Am. Chem. Soc.*, 2016, **138**, 962–968.
23 P. Chen, M. He, B. Chen and B. Hu, *Ecotoxicol. Environ. Saf.*, 2020, **205**, 111110.
24 M. Singh, A. Chakrapani and D. O'Hagon, *Expert Rev. Vaccines*, 2007, **6**, 797–808.
25 A. L. Tornesello, M. Tagliamonte, M. L. Tornesello, F. M. Buonaguro and L. Buonaguro, *Cancers*, 2020, **12**, DOI: 10.3390/cancers12041049.
26 F. Duan, X. C. Feng, X. J. Yang, W. T. Sun, Y. Jin, H. F. Liu, K. Ge, Z. H. Li and J. C. Zhang, *Biomaterials*, 2017, **122**, 23–33.
27 H. Shen, A. L. Ackerman, V. Cody, A. Giodini, E. R. Hinson, P. Cresswell, R. L. Edelson, W. M. Saltzman and D. J. Hanlon, *Immunology*, 2006, **117**, 78–88.
28 M. Y. Pei, R. Xu, C. N. Zhang, X. L. Wang, C. Li and Y. Z. Hu, *Colloids Surf., B*, 2021, **197**, DOI: 10.1016/j.colsurfb.2020.111378.
29 X. X. Liu, J. L. Liu, D. Liu, Y. F. Han, H. Y. Xu, L. X. Liu, X. G. Leng and D. L. Kong, *Biomater. Sci.*, 2019, **7**, 5516–5527.
30 G. Trinchieri, *Blood*, 1994, **84**, 4008–4027.
31 C. Qian and X. Cao, *Semin. Immunol.*, 2018, **35**, 3–11.
32 X. Ma, *Microbes Infect.*, 2001, **3**, 121–129.
33 V. Baud and M. Karin, *Trends Cell Biol.*, 2001, **11**, 372–377.
34 A. Dittrich, W. Hessenkemper and F. Schaper, *Cytokine Growth Factor Rev.*, 2015, **26**, 595–602.
35 C. S. Hsieh, S. E. Macatonia, C. S. Tripp, S. F. Wolf, A. O'Garra and K. M. Murphy, *J. Immunol.*, 2008, **181**, 4437–4439.
36 P. Kalinski, H. H. Smits, J. H. N. Schuitemaker, P. L. Vieira, M. van Eijk, E. C. de Jong, E. A. Wierenga and M. L. Kapsenberg, *J. Immunol.*, 2000, **165**, 1877–1881.
37 C. B. Maassen, W. J. Boersma, C. van Holten-Neelen, E. Claassen and J. D. Laman, *Vaccine*, 2003, **21**, 2751–2757.
38 J. P. M. Almeida, A. Y. Lin, E. R. Figueroa, A. E. Foster and R. A. Drezek, *Small*, 2015, **11**, 1453–1459.
39 W. Sang, Z. Zhang, Y. L. Dai and X. Y. Chen, *Chem. Soc. Rev.*, 2019, **48**, 3771–3810.
40 B. B. Ding, S. Shao, C. Yu, B. Teng, M. F. Wang, Z. Y. Cheng, K. L. Wong, P. A. Ma and J. Lin, *Adv. Mater.*, 2018, **30**, e1802479.

41 R. B. Smeltz, J. Chen, R. Ehrhardt and E. M. Shevach, *J. Immunol.*, 2002, **168**, 6165–6172.
42 C. Le Page, P. Genin, M. G. Baines and J. Hiscott, *Rev. Immunogenet.*, 2000, **2**, 374–386.
43 P. G. Fallon, H. E. Jolin, P. Smith, C. L. Emson, M. J. Townsend, R. Fallon, P. Smith and A. N. McKenzie, *Immunity*, 2002, **17**, 7–17.
44 A. O'Garra and K. Murphy, *Curr. Opin. Immunol.*, 1994, **6**, 458–466.